



Universiteit
Leiden
The Netherlands

Phase-shifted Andreev levels in an altermagnet Josephson junction

Beenakker, C.W.J.; Vakhtel, T.

Citation

Beenakker, C. W. J., & Vakhtel, T. (2023). Phase-shifted Andreev levels in an altermagnet Josephson junction. *Physical Review B*, 108(7). doi:10.1103/PhysRevB.108.075425

Version: Publisher's Version

License: [Leiden University Non-exclusive license](#)


Downloaded from: <https://hdl.handle.net/1887/3718615>

Note: To cite this publication please use the final published version (if applicable).

Phase-shifted Andreev levels in an altermagnet Josephson junction

C. W. J. Beenakker  and T. Vakhel 

Instituut-Lorentz, Universiteit Leiden, P.O. Box 9506, 2300 RA Leiden, The Netherlands

 (Received 3 July 2023; revised 13 August 2023; accepted 15 August 2023; published 22 August 2023)

We compute the effect of a d -wave magnetization (altermagnetism) on the spectrum of bound states (Andreev levels) in a junction between two s -wave superconductors (gap Δ_0 and phase difference ϕ). Compared to a nonmagnetic junction, the ϕ dependence of the spectrum is shifted by an offset $\pm\delta\phi$, dependent on the spin direction, so that the Andreev levels become spin polarized. In a planar junction, oriented along the crystalline axis of d_{xy} -wave symmetry, the excitation energies are determined by the normal-state transmission probability T according to $E = \Delta_0\sqrt{1 - T \sin^2(\phi \pm \delta\phi)}$. We calculate the corresponding Josephson energy and supercurrent, recovering the $0-\pi$ transition of related studies.

DOI: [10.1103/PhysRevB.108.075425](https://doi.org/10.1103/PhysRevB.108.075425)

I. INTRODUCTION

Altermagnets (metals with a d -wave magnetization that “alternates” direction in momentum space) differ from ferromagnets and antiferromagnets in that they combine a spin-polarized Fermi surface with a vanishing net magnetization [1–4]. Candidate altermagnetic materials include RuO_2 , MnTe , and Mn_5Si_3 [5–8]. The interplay of altermagnetism and superconductivity produces unusual effects [9], including orientation-dependent Andreev reflection [10,11], negative critical supercurrent with finite-momentum Cooper pairing [12,13], and topological Majorana modes [14,15].

A basic building block for these effects is the altermagnet Josephson junction in which two s -wave superconductors (gap Δ_0 , phase difference ϕ) are connected by a d -wave magnetic region (see Fig. 1). The subgap excitations are Andreev levels, electron-hole superpositions confined to the junction. If the length L of the junction is short compared to the superconducting coherence length $\xi_0 = \hbar v_F/\Delta_0$, there is one Andreev level per spin direction and per transverse mode.

For a nonmagnetic Josephson junction, the Andreev levels are spin degenerate, and the ϕ dependence of the excitation energy is given by [16]

$$E = \Delta_0\sqrt{1 - T \sin^2(\phi/2)}, \quad (1.1)$$

where $T \in (0, 1)$ is the transmission probability through the junction of an electron mode at the Fermi level in the normal state.

Here, we investigate how the altermagnet modifies the excitation spectrum. For unit transmission through a planar junction the $\cos(\phi/2)$ Andreev band is split into spin-polarized branches. The splitting is a phase-shift $\pm\delta\phi$ that depends on the angle θ of the junction with the crystalline axis of d_{xy} -wave symmetry. For $\theta = 0$, the relation (1.1) with $\phi \mapsto \phi \pm \delta\phi$ still holds for nonunit transmission. We test these analytical predictions with a computer simulation of a tight-binding model of the altermagnet Josephson junction.

These results provide an alternative description of the $0-\pi$ transition reported recently [12,13] where the sign of the critical current oscillates with increasing L . The description is particularly simple for $\theta = 0$ when the phase-shift $\delta\phi$ is proportional to the transverse momentum k_y , so $\partial E/\partial\phi \propto \partial E/\partial k_y$. The supercurrent $I \propto \int_{-k_F}^{k_F} dk_y (dE/d\phi)$ is, therefore, directly given by an energy difference—the integral operation cancels the derivative. The resulting critical current I_c oscillates $\propto (\sin \delta\phi_{\max})/\delta\phi_{\max}$, with $\delta\phi_{\max} \propto k_F L$.

II. ALTERMAGNET JOSEPHSON JUNCTION

We consider the Josephson junction geometry of Fig. 1, consisting of a pair of superconducting regions ($x < 0$ and $x > L$) connected by a nonsuperconducting magnetic metal ($0 < x < L$). The superconducting pair potential Δ has s -wave symmetry, whereas, the magnetization has the d -wave symmetry characteristic of an altermagnet. The junction has length L and width W .

For large width W , and without impurity scattering, we may assume translational invariance in the y direction so that the transverse momentum k_y is a good quantum number. We work in the short-junction regime $L \ll \xi_0$.

The excitation spectrum is described by the Bogoliubov–de Gennes (BdG) Hamiltonian,

$$\mathcal{H}(\mathbf{k}) = \begin{pmatrix} H_0(\mathbf{k}) & \Delta \\ \Delta^* & -\sigma_y H_0^*(-\mathbf{k})\sigma_y \end{pmatrix}, \quad (2.1)$$

$$H_0(\mathbf{k}) = \frac{\hbar^2}{2m}(k_x^2 + k_y^2) - \mu + \frac{\hbar^2}{m}t_1 k_x k_y \sigma_z + \frac{\hbar^2}{m}t_2(k_y^2 - k_x^2)\sigma_z. \quad (2.2)$$

The σ_α 's are Pauli spin matrices, $\mathbf{k} = (k_x, k_y)$ is the electron momentum (two dimensional, for simplicity), and $\mu = \hbar^2 k_F^2/2m = \frac{1}{2}mv_F^2$ is the Fermi energy. In what follows, we set $\hbar = 1$ and the electron mass $m = 1$ (restoring units in the final results).

The d -wave exchange interaction is characterized by two dimensionless parameters t_1 and t_2 , which depend on angle θ

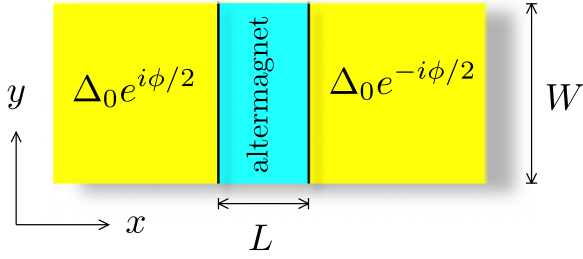


FIG. 1. Josephson junction consisting of a pair of superconductors (pair potential Δ_0 , phase difference ϕ) connected by an altermagnet. We consider a short planar junction $W \gg \xi_0 \gg L$.

of the altermagnet-superconductor (AS) interface relative to the crystalline axes,

$$t_1 = 2t_0 \cos 2\theta, \quad t_2 = t_0 \sin 2\theta. \quad (2.3)$$

The parameter t_0 is on the order of 10^{-1} [8]. For $\theta = 0$, the magnetization has pure d_{xy} -wave symmetry for $\theta = \pi/4$, it has pure $d_{x^2-y^2}$ -wave symmetry.

The 4×4 Hamiltonian (2.1) decouples into 2×2 blocks \mathcal{H}_\uparrow and \mathcal{H}_\downarrow . The blocks are spin polarized in the sense that electrons and holes occupy opposite spin bands so that each block describes quasiparticles with a definite magnetic moment.

We consider the spin-up block,

$$\mathcal{H}_\uparrow(\mathbf{k}) = \begin{pmatrix} H_+(\mathbf{k}) & \Delta \\ \Delta^* & -H_-(\mathbf{k}) \end{pmatrix}, \quad (2.4)$$

$$H_\pm(\mathbf{k}) = \frac{1}{2}(k_x^2 + k_y^2) - \mu \pm t_1 k_x k_y \pm t_2 (k_y^2 - k_x^2). \quad (2.5)$$

The spin-down block \mathcal{H}_\downarrow is obtained by switching $t_1 \mapsto -t_1$, $t_2 \mapsto -t_2$.

Near the Fermi level ($E = 0$), we may linearize the k_x dependence of \mathcal{H}_\uparrow at given momentum k_y , parallel to the AS interfaces at $x = 0$ and $x = L$. In the altermagnet region $0 < x < L$, where $\Delta = 0$, we have

$$\mathcal{H}_\uparrow = (\bar{v} - \tau_z \delta v) v_z \tau_z (k_x - Q_0 - Q_z \tau_z). \quad (2.6)$$

The Pauli matrix τ_z acts on the electron-hole degree of freedom, whereas, v_z distinguishes right movers from left movers.

In Eq. (2.6), we have introduced the velocities,

$$v_\pm = v_F \sqrt{1 \pm 2t_2 - (k_y/k_F)^2 (1 - t_1^2 - 4t_2^2)} \equiv \bar{v} \pm \delta v, \quad (2.7)$$

and momentum offsets

$$Q_0 = k_F (1 - 4t_2^2)^{-1} [v_z (\bar{v} - 2t_2 \delta v) / v_F - 2t_1 t_2 k_y / k_F],$$

$$Q_z = k_F (1 - 4t_2^2)^{-1} [v_z (2t_2 \bar{v} - \delta v) / v_F - t_1 k_y / k_F]. \quad (2.8)$$

For later use, we also define

$$Q_0^\pm = k_F (1 - 4t_2^2)^{-1} [\pm (\bar{v} - 2t_2 \delta v) / v_F - 2t_1 t_2 k_y / k_F],$$

$$Q_z^\pm = k_F (1 - 4t_2^2)^{-1} [\pm (2t_2 \bar{v} - \delta v) / v_F - t_1 k_y / k_F]. \quad (2.9)$$

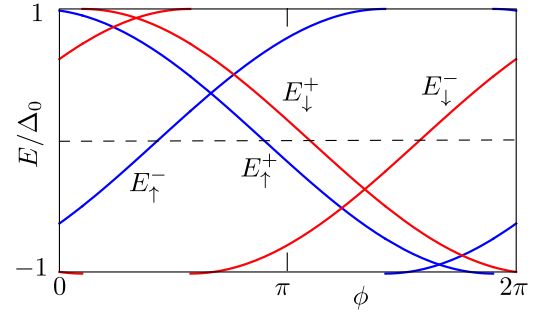


FIG. 2. Phase dependence of the Andreev levels, computed from Eq. (3.3) for $t_1 = t_2 = 0.1$, $k_F L = 20$, $k_y/k_F = 1/2$. There are four levels at each value of the phase difference, distinguished by the spin direction \uparrow, \downarrow and by the \pm sign of the current $\propto dE/d\phi$, which they carry. Another four levels at $k_y/k_F = -1/2$ ensures the electron-hole symmetry of the spectrum. Normal reflections are neglected in this calculation.

III. ANDREEV LEVELS WITHOUT NORMAL REFLECTION

Andreev reflection at $x = 0$ and $x = L$ converts electrons into holes, with absorption of the missing charge of $2e$ into the superconducting condensate [17]. It coexists with normal reflection without charge conversion. In this section, we neglect normal reflections, we will include these in the next section.

Andreev reflection from electron to hole with energy E , at a pair potential $\Delta = \Delta_0 e^{i\phi}$, is associated with a phase-shift $e^{-i\phi - i\alpha(E)}$, where

$$\alpha(E) = \arccos(E/\Delta_0) \in (0, \pi), \quad |E| < \Delta_0. \quad (3.1)$$

The phase shift for reflection from hole to electron is $e^{+i\phi - i\alpha(E)}$. We set $\Delta = \Delta_0 e^{i\phi/2}$ at the left-superconductor ($x < 0$) and $\Delta = \Delta_0 e^{-i\phi/2}$ at the right-superconductor ($x > L$).

The condition for a bound state is that the phase increment on a round-trip $x = 0 \mapsto L \mapsto 0$ is a multiple of 2π . For $k_F L \ll \mu/\Delta_0$ (equivalently, $L \ll \xi_0$, the short-junction regime) we may ignore the energy dependence of the phase shift accumulated in the normal region, whereas, retaining the energy dependence of the Andreev reflection phase-shift $\alpha(E)$. This gives the bound-state condition,

$$\phi + 2LQ_z^\pm = \pm 2\alpha(E) \pmod{2\pi}. \quad (3.2)$$

The \pm sign distinguishes whether the right-moving quasiparticle is an electron or a hole. The contribution Q_0 to the phase shift cancels in the round trip, only the increment Q_z contributes.

We, thus, obtain two branches of Andreev levels E_\uparrow^\pm , with

$$E_\uparrow^\pm = \pm \Delta_0 \operatorname{sgn}(\sin \psi_\uparrow^\pm) |\cos \frac{1}{2} \psi_\uparrow^\pm|, \quad (3.3a)$$

$$\psi_\uparrow^\pm = \phi + 2LQ_z^\pm. \quad (3.3b)$$

We have added the subscript \uparrow as a reminder that these are the bound states of \mathcal{H}_\uparrow . For \mathcal{H}_\downarrow , one replaces $L \mapsto -L$.

In a nonmagnetic Josephson junction, the Andreev levels are spin degenerate with a cosine phase dependence [18]: $E = \pm \Delta_0 \cos(\phi/2)$. As illustrated in Fig. 2, the altermagnet breaks up the cosine into branches that are phase shifted by

a spin-dependent amount. Each branch connects the edges of the gap at $\pm\Delta_0$ where the bound states merge with the continuous spectrum. Electron-hole symmetry ($\pm E$ symmetry of the spectrum) is ensured by the identity,

$$Q_z^+(k_y) = -Q_z^-(k_y) \Rightarrow E_{\uparrow}^{\pm}(k_y) = -E_{\downarrow}^{\mp}(-k_y). \quad (3.4)$$

IV. INCLUDING NORMAL REFLECTION

An electron incident on the superconductor may be Andreev reflected as a hole, but it may also be reflected as an electron. Such normal reflection can be modeled by the insertion of a tunnel barrier at the two ends of the altermagnet. We assume that the barrier potential $V(x)$ does not break the translational invariance along the y direction so that the transverse momentum k_y remains a good quantum number. We also assume the potential is spin independent.

A simple solution of the scattering problem is possible for pure d_{xy} -wave pairing ($t_2 = 0$). The BdG Hamiltonian then reads

$$\mathcal{H} = \left[\frac{1}{2}k_x^2 + \frac{1}{2}k_y^2 + V(x) - \mu \right] \tau_z + \frac{1}{2} [t_1(x)k_x + k_x t_1(x)] k_y \sigma_z + \Delta_0(x) [\tau_x \cos \phi(x) - \tau_y \sin \phi(x)]. \quad (4.1)$$

The x dependence of the magnetization and pair potential is included to describe the entire junction profile. The anticommutator of $t_1(x)$ and k_x ensures the Hermiticity of \mathcal{H} [10].

We make the unitary transformation $\mathcal{H} \mapsto U(x)\mathcal{H}U^\dagger(x)$ with

$$U(x) = \exp\left(i\tau_z \sigma_z k_y \int_0^x t_1(x') dx'\right), \quad (4.2)$$

resulting in

$$\mathcal{H} = \left[\frac{1}{2}k_x^2 + \frac{1}{2}(1 - t_1^2)k_y^2 + V(x) - \mu \right] \tau_z + \Delta_0(x) [\tau_x \cos \tilde{\phi}(x) - \tau_y \sin \tilde{\phi}(x)], \quad (4.3)$$

where $\tilde{\phi}(x) = \phi(x) + 2\sigma_z k_y \int_0^x t_1(x') dx'$ is a spin-dependent phase difference.

So for a given k_y and given spin direction, the altermagnet Josephson junction is equivalent to a nonmagnetic Josephson junction with phase difference $\phi \pm 2k_y L t_1$. The factor $1 - t_1^2$ that multiplies k_y^2 in Eq. (4.3) amounts to an anisotropic mass, this factor can be set to unity for $t_1 \ll 1$. We can, then, use the known result (1.1) for the Andreev levels in a nonmagnetic Josephson junction,

$$E_{\uparrow}^{\pm}(k_y) = \pm \Delta_0 \sqrt{1 - T(k_y) \sin^2(\phi/2 - k_y L t_1)},$$

$$E_{\downarrow}^{\pm}(k_y) = \pm \Delta_0 \sqrt{1 - T(k_y) \sin^2(\phi/2 + k_y L t_1)}, \quad (4.4)$$

where $T(k_y)$ is the transmission probability through the junction in the normal-state ($\Delta_0 = 0$).

If t_2 is nonzero, we do not have such a closed-form and general expression for the Andreev levels. We specify to the case of a tunnel barrier at each AS interface with tunnel probability Γ (the same at $x = 0$ and at $x = L$). The scattering matrix calculation in Appendix A gives the spin-up Andreev levels E_{\uparrow}^{\pm} as the two solutions of the nonlinear equation,

$$(1 - \Gamma)^2 \cos[2\alpha(E) + L(Q_z^+ - Q_z^-)] + \cos[2\alpha(E) - L(Q_z^+ - Q_z^-)] - \Gamma^2 \cos[\phi + L(Q_z^+ + Q_z^-)]$$

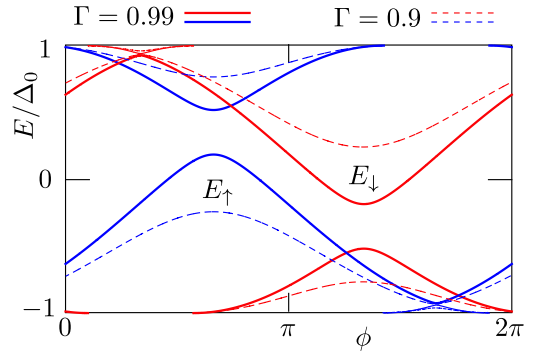


FIG. 3. Same as Fig. 2, but now including normal reflections at each AS interface. The spectra are calculated from Eq. (4.5) for two values of the transmission probability Γ , at $t_1 = t_2 = 0.1$, $k_F L = 20$, $k_y/k_F = 1/2$.

$$= 2(1 - \Gamma) \cos[L(Q_z^+ - Q_z^-)] + 4(1 - \Gamma) \times \cos[L(Q_0^+ - Q_0^-)] (1 - E^2/\Delta_0^2). \quad (4.5)$$

The spin-down Andreev levels E_{\downarrow}^{\pm} are the solutions of Eq. (4.5) upon replacement of L by $-L$.

As a check, if we now set $t_2 = 0$, we have $Q_z^+ = Q_z^-$, $Q_0^+ = -Q_0^-$, and Eq. (4.5) has the solution (4.4) with

$$T(k_y) = \frac{\Gamma^2}{2(1 - \Gamma) \cos 2LQ_0^+ + 1 + (1 - \Gamma)^2}. \quad (4.6)$$

This is indeed the normal-state transmission probability through a double-barrier junction, at momentum $Q_0^+ = \sqrt{k_F^2 - (1 - t_1^2)k_y^2}$.

If $t_2 \neq 0$, Eq. (4.5) can readily be solved numerically. As illustrated in Fig. 3, crossings in the spectrum between levels of the same spin become anticrossings.

V. COMPARISON WITH COMPUTER SIMULATIONS

To test these analytical predictions, we have discretized the BdG Hamiltonian (2.2) on a square lattice and computed the subgap excitation spectrum numerically (see Appendix B). These computer simulations fully include the normal reflections at the AS interfaces, and they do not rely on the short-junction approximation.

In Fig. 4, we compare with the analytical predictions that ignore normal reflection. As expected, the main effect of normal reflection at the AS interfaces is to transform the crossings between same-spin branches into anticrossings. The effect is most pronounced when t_1 and t_2 are both nonzero: In the two cases of pure d_{xy} -wave or pure $d_{x^2-y^2}$ -wave magnetization the crossings are only weakly affected.

In Fig. 5, we test the relation (4.4) between the Andreev levels and the normal-state transmission probability in the case of d_{xy} -wave pairing. The agreement is quite good without any adjustable parameter.

VI. JOSEPHSON ENERGY AND SUPERCURRENT

The supercurrent in the short-junction regime is carried entirely by the bound states, the continuous spectrum does not

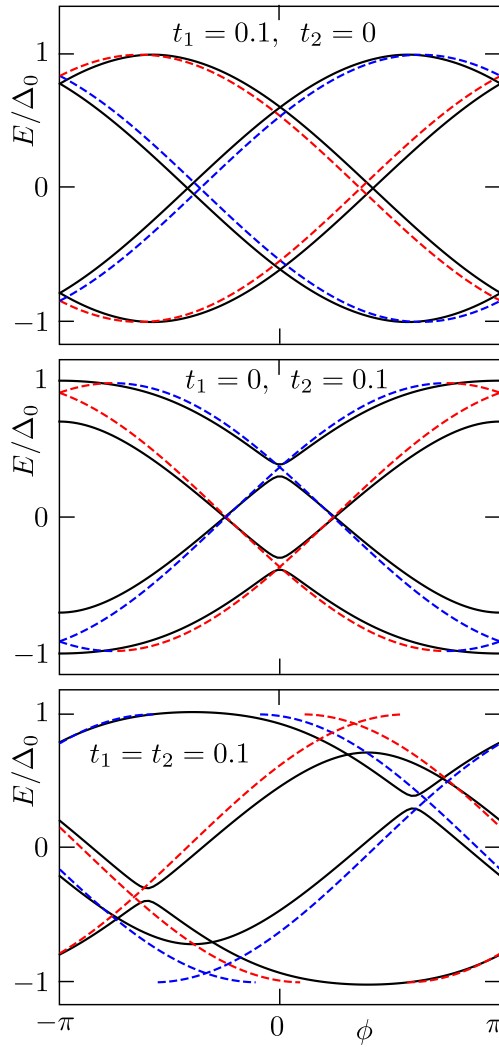


FIG. 4. Andreev level spectra in the altermagnet Josephson junction for $k_F L = 20$, $k_y/k_F = 1/2$, and different choices of t_1, t_2 . The solid curves result from the numerical solution of the BdG equation on a lattice. The dashed curves are the analytical predictions (3.3) in which normal reflections at the AS interfaces are neglected (blue for spin up, red for spin down).

contribute [16,19,20]. In equilibrium at inverse temperature β , the supercurrent I is given by the phase derivative of the Josephson energy F ,

$$I = \frac{2e}{\hbar} \frac{d}{d\phi} F, \quad F = - \sum_{E>0} \frac{1}{2} E \tanh\left(\frac{1}{2}\beta E\right), \quad (6.1)$$

where $\sum_{E>0}$ is a sum over the transverse momentum k_y and spin \uparrow, \downarrow of the Andreev levels in the interval $(0, \Delta_0)$.

In the absence of normal reflections, we find from Eqs. (3.3) and (3.4) that

$$F = - \sum_{k_y} \sum_{s=\pm} \frac{1}{2} \varepsilon_s \Delta_0 \tanh\left(\frac{1}{2}\varepsilon_s \beta \Delta_0\right), \quad (6.2a)$$

$$\varepsilon_s = |\cos(\phi/2 + sLQ_c^+)|. \quad (6.2b)$$

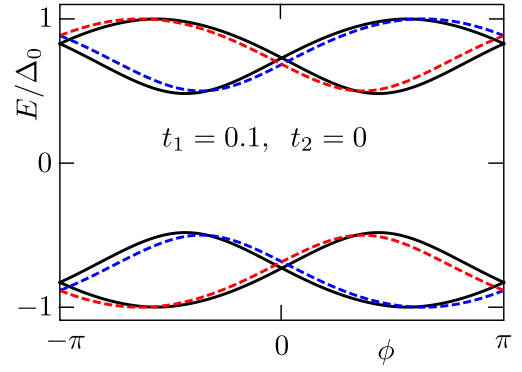


FIG. 5. Solid curves: Andreev levels for d_{xy} -wave pairing in the presence of a tunnel barrier at the two AS interfaces ($k_F L = 20$, $k_y/k_F = 1/2$). The normal-state transmission probability $T = 0.75$ through the junction was obtained directly from the computer simulation (by setting $\Delta_0 \equiv 0$). The dashed curves are the analytical prediction (4.4) for the same value of T (blue for spin up, red for spin down).

The transverse momenta range over the interval $(-k_{\max}, k_{\max})$ with

$$k_{\max} = k_F \sqrt{\frac{1 - 2t_2}{1 - t_1^2 - 4t_2^2}}, \quad (6.3)$$

in view of Eq. (2.7). In a junction of width $W \gg L, \xi_0$, and at zero temperature, one has

$$I(\phi) = - \frac{e\Delta_0 W}{\hbar} \frac{1}{2\pi} \int_{-k_{\max}}^{k_{\max}} dk_y \frac{d}{d\phi} (\varepsilon_+ + \varepsilon_-). \quad (6.4)$$

The integral over k_y in Eq. (6.4) can be carried out in closed form for the case $t_2 = 0$ of a pure d_{xy} -wave magnetization when $\varepsilon_s = |\cos(\phi/2 - st_1 k_y L)|$. We find

$$I = \frac{I_0}{2\alpha} (|\cos(\phi/2 - \alpha)| - |\cos(\phi/2 + \alpha)|), \quad (6.5)$$

with $I_0 = (e\Delta_0/\hbar)(k_{\max} W/\pi)$ and $\alpha = t_1 k_{\max} L$.

The critical current from Eq. (6.5) is given by

$$I_c = I_0 \frac{\sin 2\alpha}{2\alpha}, \quad (6.6)$$

see Fig. 6. A negative sign of I_c means that the maximum supercurrent is reached in the interval $-\pi < \phi < 0$. When $I_c < 0$, the Josephson energy is minimal at $\phi = \pi$ rather than at $\phi = 0$, the altermagnet Josephson junction has become a π junction [12,13].

With increasing L , a negative critical current first appears in the interval $\pi/2 < t_1 k_{\max} L < \pi$. At $L = L^* \equiv 3\pi/(4t_1 k_{\max})$, one has $I_c = -(2/3)I_0$, so the negative I_c is comparable in magnitude to the value I_0 at $L = 0$. Note that this characteristic length L^* is still in the short-junction regime provided that t_1 is not too small, we need $\Delta_0/\mu \ll t_1 \ll 1$.

These results are not changed qualitatively if we include a $d_{x^2-y^2}$ contribution to the magnetization, see Fig. 7. In the case of $t_1 = 0$ of a pure $d_{x^2-y^2}$ -wave magnetization, the negative critical current first appears in the interval $\pi/2 < \tilde{t}_2 k_{\max} L < \pi$ with

$$\tilde{t}_2 = \frac{1}{2}(1 - 2t_2)^{-1/2} - \frac{1}{2}(1 + 2t_2)^{-1/2} = t_2 + O(t_2^2). \quad (6.7)$$

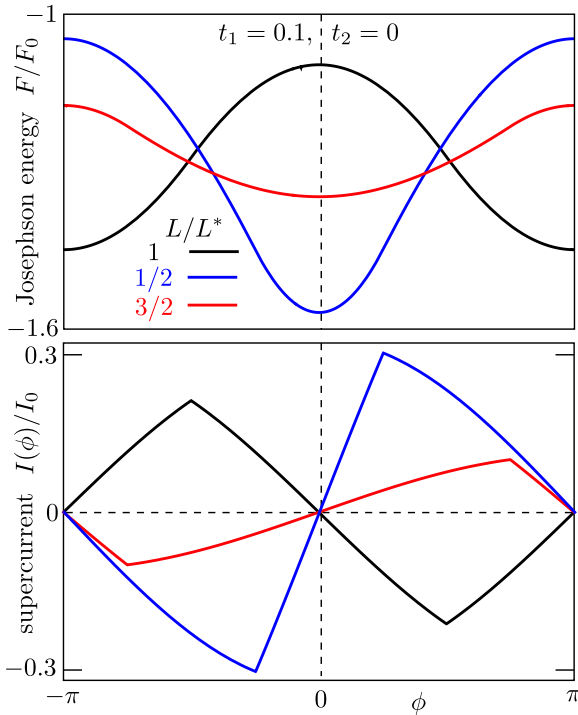


FIG. 6. Phase dependence of the Josephson energy (top panel in units of $F_0 = \Delta_0 k_{\max} W / \pi$) and the supercurrent [lower panel, in units of $I_0 = (e/\hbar)F_0$] in the altermagnet Josephson junction for different lengths L of the junction [in units of $L^* = 3\pi/(4t_1 k_{\max})$]. In the interval $2/3 < L/L^* < 4/3$ the Josephson energy is maximal rather than minimal at $\phi = 0$, resulting in a negative critical current. These are results for pure d_{xy} -wave magnetization ($t_2 = 0$) and without normal reflection ($\Gamma = 1$).

All of this was without normal reflections. We consider the effect of a tunnel barrier (transmission probability Γ) at each AS interface in the case of pure d_{xy} -wave magnetization when we have the closed-form expression (4.4) for the Andreev levels. As illustrated in Fig. 8, the barrier reduces the magnitude of the critical current, but its sign remains unchanged. For $\Gamma \ll 1$ the critical current (6.6) is reduced by a factor Γ

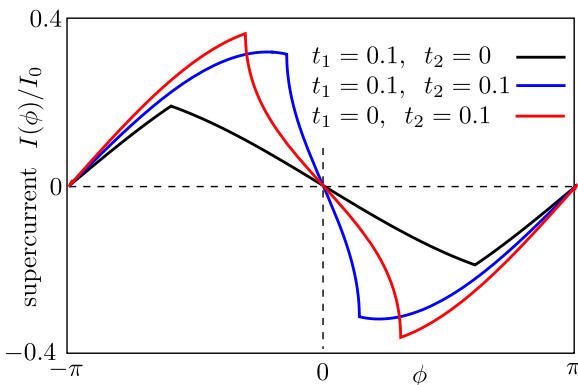


FIG. 7. Current-phase relationship for the case of pure d_{xy} -wave magnetization (black, $t_2 = 0$, $t_1 = 0.1$, and $k_F L = 25$), pure $d_{x^2-y^2}$ -wave magnetization (red, $t_1 = 0$, $t_2 = 0.1$, and $k_F L = 20$) and the equal weight case (blue, $t_1 = t_2 = 0.1$, $k_F L = 15$).

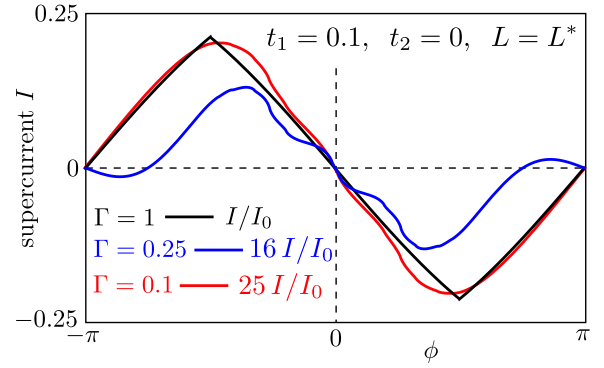


FIG. 8. The black curve shows the supercurrent (6.5) without normal reflections, the blue and red curves include normal reflections from a barrier at each AS interface [transmission probability Γ , Andreev levels given by Eqs. (4.4) and (4.6)]. Each curve is for the same junction length $L = L^*$ and d_{xy} magnetization strength $t_1 = 0.1$ (with $t_2 = 0$).

because only the transmission resonance peaks (unit height and width Γ) contribute.

We can compare our analytical result (6.5) for the supercurrent-phase relationship with Ref. [13], which studies the same system in a different formulation. (The numerical study of Ref. [12] does not contain results that can be directly compared with ours.) Although qualitatively, we find the same sign changes in the critical current with increasing L , the decay rate of the oscillations is different in Ref. [13]: $I_c \propto L^{-3/2}$ instead of the $1/L$ decay in Eq. (6.6). Moreover, Eq. (6.5) is strongly nonsinusoidal, whereas, Ref. [13] finds $I(\phi) \propto \sin \phi$. The absence of higher harmonics suggests a perturbative approximation ($\Gamma \ll 1$). We emphasize that our result is fully nonperturbative.

VII. CONCLUSION

To summarize, we have extended the scattering theory of nonmagnetic Josephson junctions to the case of an altermagnetic junction. The basic effect of the d -wave magnetization is to spin polarize the Andreev levels by giving the spin-up and spin-down spectra $E(\phi)$ opposite phase-shifts $\pm \delta \phi$.

For a planar junction aligned along the crystalline axes of d_{xy} -wave symmetry, the phase shift is proportional to the transverse momentum k_y , which upon integration of $dE/d\phi$ over k_y gives the simple closed-form result (6.5) for the supercurrent.

As noticed previously [12,13], the altermagnet Josephson junction undergoes 0- π transitions with increasing junction length L where the critical current changes sign. Our approach is nonperturbative in the transmission probability through the junction, producing the strongly nonsinusoidal current-phase relationship of Figs. 6 and 7. To observe this the junction length, L should be below the superconducting coherence length ξ_0 and also below the mean free path l for impurity scattering. The characteristic value of L for a negative critical current is $3\pi/(4t_1 k_F)$, which for $t_1 \simeq 0.1$ and $k_F \simeq 10^9 \text{ m}^{-1}$ amounts to a realistically short junction length of $L \simeq 20 \text{ nm}$.

ACKNOWLEDGMENTS

This project has received funding from the European Research Council (ERC) under the European Union's Horizon 2020 Research and Innovation Programme. Advice from A. R. Akhmerov, B. van Heck, and G. Lemut has been very helpful.

APPENDIX A: SCATTERING MATRIX CALCULATION OF THE ANDREEV LEVELS

We consider the altermagnet Josephson junction of Fig. 1 with a tunnel barrier (transmission probability Γ) at $x = 0$ and $x = L$. We calculate the Andreev level spectrum by means of the scattering formulation of Ref. [16].

The scattering matrix $S(E)$ of electrons (e) and holes (h) at energy E , incident on the altermagnet from the left (L) or the right (R) with transverse momentum k_y , has the block-diagonal form

$$S(E) = \begin{pmatrix} S_e(E) & 0 \\ 0 & S_h(E) \end{pmatrix}, \quad (\text{A1})$$

$$\Psi_{\text{out}} = S\Psi_{\text{in}}, \quad \Psi = (\psi_{e,L}, \psi_{e,R}, \psi_{h,L}, \psi_{h,R}). \quad (\text{A2})$$

Without the tunnel barrier and at the Fermi level ($E = 0$) one would have simply

$$S_e(0) = \begin{pmatrix} 0 & \exp(-iL[Q_0^- + Q_z^-]) \\ \exp(iL[Q_0^+ + Q_z^+]) & 0 \end{pmatrix}, \quad (\text{A3a})$$

$$S_h(0) = \begin{pmatrix} 0 & \exp(-iL[Q_0^+ - Q_z^+]) \\ \exp(iL[Q_0^- - Q_z^-]) & 0 \end{pmatrix}, \quad (\text{A3b})$$

in terms of the momentum offsets defined in Eq. (2.9).

Multiple reflections by the two barriers change this into

$$S_e(0) = \frac{1}{1 + (1 - \Gamma)e^{iLK_e}} \times \begin{pmatrix} \sqrt{1 - \Gamma}(1 + e^{iLK_e}) & \Gamma \exp(-iL[Q_0^- + Q_z^-]) \\ \Gamma \exp(iL[Q_0^+ + Q_z^+]) & -\sqrt{1 - \Gamma}(1 + e^{iLK_e}) \end{pmatrix}, \quad (\text{A4a})$$

$$K_e = Q_0^+ - Q_0^- + Q_z^+ - Q_z^-, \quad (\text{A4b})$$

$$S_h(0) = \frac{1}{1 + (1 - \Gamma)e^{iLK_h}} \times \begin{pmatrix} \sqrt{1 - \Gamma}(1 + e^{iLK_h}) & \Gamma \exp(-iL[Q_0^+ - Q_z^+]) \\ \Gamma \exp(iL[Q_0^- - Q_z^-]) & -\sqrt{1 - \Gamma}(1 + e^{iLK_h}) \end{pmatrix}, \quad (\text{A4c})$$

$$K_h = -Q_0^+ + Q_0^- + Q_z^+ - Q_z^-. \quad (\text{A4d})$$

We set $\Delta = \Delta_0 e^{i\phi/2}$ at the left superconductor ($x < 0$) and $\Delta = \Delta_0 e^{-i\phi/2}$ at the right superconductor ($x > L$). The condition for a bound state is

$$\text{Det}[1 - R(E)S(E)] = 0, \quad (\text{A5})$$

in terms of the scattering matrix $S(E)$ of the normal region and the Andreev reflection matrix,

$$R(E) = e^{-i\alpha(E)} \begin{pmatrix} 0 & R_{eh} \\ R_{he} & 0 \end{pmatrix}, \quad R_{eh} = R_{he}^* = \begin{pmatrix} e^{i\phi/2} & 0 \\ 0 & e^{-i\phi/2} \end{pmatrix}. \quad (\text{A6})$$

The function $\alpha(E)$, given by Eq. (3.1), varies on the scale of Δ_0 . The energy scale on which $S(E)$ varies is on the order of $\Gamma\bar{v}/L$. If $L \ll \Gamma\bar{v}/\Delta_0$, it is consistent to evaluate $S(E)$ at $E = 0$, whereas, retaining the energy dependence of $R(E)$.

Substitution of of Eqs. (A4) and (A6) into Eq. (A5) gives the determinantal equation (4.5) from the main text.

APPENDIX B: TIGHT-BINDING CALCULATIONS

For the computer simulations, we discretized the altermagnet Hamiltonian (2.2) on a square lattice (lattice constant a , mass m , and \hbar all set to unity),

$$H_0 = 2 - \cos k_x - \cos k_y - \mu + t_1 \sin k_x \sin k_y \sigma_z + 2t_2(\cos k_x - \cos k_y)\sigma_z. \quad (\text{B1})$$

In the two superconducting regions, we set $t_1 = 0 = t_2$ and couple the electron and hole blocks by a pair potential $\Delta_0 e^{\pm i\phi/2}$. We keep the same chemical potential μ throughout.

The system is infinitely extended in the y direction. In the x direction, the altermagnet is in the interval $0 < x < L$, whereas, the superconductors occupy the regions $-L_S < x < 0$ and $L < x < L_S$. The length L_S is chosen much larger than the superconducting coherence length $\xi_0 = \sqrt{2\mu}/\Delta_0$. We took $\mu = 0.5$ and $\Delta_0 = 5 \times 10^{-4}$, hence, $\xi_0 = 2000$. With $L = 20$, we are, therefore, deep in the short-junction regime. The tight-binding model is implemented by means of the Kwant toolbox [21].

For Fig. 5, we inserted a tunnel barrier at $x = 0$ and $x = L$ by locally modifying the hopping matrix elements. The transmission probability T through the junction was calculated separately for $\Delta_0 = 0$ so that there are no adjustable parameters in the comparison with the analytics.

- [1] L. Šmejkal, J. Sinova, and T. Jungwirth, Beyond Conventional Ferromagnetism and Antiferromagnetism: A Phase with Non-relativistic Spin and Crystal Rotation Symmetry, *Phys. Rev. X* **12**, 031042 (2022).
 [2] L. Šmejkal, J. Sinova, and T. Jungwirth, Emerging Research Landscape of Altermagnetism, *Phys. Rev. X* **12**, 040501 (2022).
 [3] I. I. Mazin, Altermagnetism—a New Punch Line of Fundamental Magnetism, *Phys. Rev. X*, **12**, 040002 (2022).

- [4] I. I. Mazin, Altermagnetism in MnTe: Origin, predicted manifestations, and routes to detwinning, *Phys. Rev. B* **107**, L100418 (2023).
 [5] Z. Feng, X. Zhou, L. Šmejkal, L. Wu, Z. Zhu, H. Guo, R. González-Hernández, X. Wang, H. Yan, P. Qin, X. Zhang, H. Wu, H. Chen, Z. Xia, C. Jiang, M. Coey, J. Sinova, T. Jungwirth, and Z. Liu, An anomalous Hall effect in altermagnetic ruthenium dioxide, *Nat. Electron.* **5**, 735 (2022).

- [6] C. A. Occhialini, L. G. P. Martins, S. Fan, V. Bisogni, T. Yasunami, M. Musashi, M. Kawasaki, M. Uchida, R. Comin, and J. Pellicciari, Strain-modulated anisotropic electronic structure in superconducting RuO₂ films, *Phys. Rev. Mater.* **6**, 084802 (2022).
- [7] R. D. Gonzalez Betancourt, J. Zubáč, R. González-Hernández, K. Geishendorf, Z. Šobán, G. Springholz, K. Olejník, L. Šmejkal, J. Sinova, T. Jungwirth, S. T. B. Goennenwein, A. Thomas, H. Reichlová, J. Železný, and D. Kriegner, Spontaneous Anomalous Hall Effect Arising from an Unconventional Compensated Magnetic Phase in a Semiconductor, *Phys. Rev. Lett.* **130**, 036702 (2023).
- [8] L. Šmejkal, A. B. Hellenes, R. González-Hernández, J. Sinova, and T. Jungwirth, Giant and Tunneling Magnetoresistance in Unconventional Collinear Antiferromagnets with Nonrelativistic Spin-Momentum Coupling, *Phys. Rev. X* **12**, 011028 (2022).
- [9] I. I. Mazin, Notes on altermagnetism and superconductivity, [arXiv:2203.05000](https://arxiv.org/abs/2203.05000).
- [10] C. Sun, A. Brataas, and J. Linder, Andreev reflection in altermagnets, *Phys. Rev. B* **108**, 054511 (2023).
- [11] M. Papaj, Andreev reflection at altermagnet/superconductor interface, [arXiv:2305.03856](https://arxiv.org/abs/2305.03856).
- [12] J. A. Ouassou, A. Brataas, and J. Linder, dc Josephson Effect in Altermagnets, *Phys. Rev. Lett.* **131**, 076003 (2023).
- [13] S.-B. Zhang, L.-H. Hu, and T. Neupert, Finite-momentum Cooper pairing in proximitized altermagnets, [arXiv:2302.13185](https://arxiv.org/abs/2302.13185).
- [14] D. Zhu, Z.-Y. Zhuang, Z. Wu, and Z. Yan, Topological superconductivity in two-dimensional altermagnetic metals, [arXiv:2305.1047](https://arxiv.org/abs/2305.1047).
- [15] S. A. A. Ghorashi, T. L. Hughes, and J. Cano, Altermagnetic routes to Majorana modes in zero net magnetization, [arXiv:2306.09413](https://arxiv.org/abs/2306.09413).
- [16] C. W. J. Beenakker, Universal Limit of Critical-Current Fluctuations in Mesoscopic Josephson Junctions, *Phys. Rev. Lett.* **67**, 3836 (1991).
- [17] A. F. Andreev, Thermal conductivity of the intermediate state of superconductors, *Sov. Phys. JETP* **19**, 1228 (1964).
- [18] I. O. Kulik and A. N. Omel'yanchuk, Properties of superconducting microbridges in the pure limit, *Sov. J. Low Temp. Phys.* **3**, 459 (1977).
- [19] C. W. J. Beenakker, *Three "Universal" Mesoscopic Josephson Effects*, in Springer Series in Solid-State Sci. Vol. 109 (Springer, Berlin/Heidelberg, 1992).
- [20] Our analysis applies to a symmetric Josephson junction, where the superconductors on both sides of the interface have the same gap Δ_0 . In a strongly asymmetric junction one would also need to include contributions to the supercurrent from the continuous spectrum, see L.-F. Chang and P. F. Bagwell, Ballistic Josephson-current flow through an asymmetric superconductor-normal-metal-superconductor junction, *Phys. Rev. B* **49**, 15853 (1994).
- [21] C. W. Groth, M. Wimmer, A. R. Akhmerov, and X. Waintal, Kwant: A software package for quantum transport, *New J. Phys.* **16**, 063065 (2014).